Growth and characterization of $(InSb)_m(InP)_n$ short period superlattices

T. Utzmeier,[a] G. Armelles, P. A. Postigo, and F. Briones
Instituto de Microelectrónica de Madrid, CSIC, Isaac Newton 8, 28760 Tres Cantos, Spain

P. Castrillo
Departamento E. y Electrónica, Dr. Mergelina s/n, 47011 Valladolid, Spain

A. Sanz-Hervas, M. Aguilar, and E. J. Abril[b]
Departamento Tecnología Electrónica, ETSIT, Ciudad Universitaria, 28040 Madrid, Spain

(Received 25 November 1996; accepted for publication 3 April 1997)

Short period superlattices of $(InSb)_m(InP)_n$ were grown on semi-insulating (001) InP substrates by atomic layer molecular beam epitaxy. High resolution x-ray diffractometry was used to study the structural quality of the superlattices. Raman spectroscopy, in conjunction with theoretical calculations, provided information about intermixing at the interfaces. © *1997 American Institute of Physics.* [S0003-6951(97)02422-4]

Renewed interest in narrow band gap III–V semiconductors like InSb, InAs, or InAsSb has come up in the recent years. These materials are especially interesting for high performance, optoelectronic applications in the infrared up to 12 μm (Ref. 1) and for magnetic field sensors. Heterostructures based on InSbP would be very useful for quantum well lasers, detectors,[2] and two-dimensional electron-gas devices.[3] Since $InSb_xP_{1-x}$, exhibits severe growth problems,[4] however, we studied the growth of short period strained layer superlattices (SPSLs) as alternative materials that could replace the ternary alloys. Nevertheless, the growth of such InSb/InP SPSLs could be, in principle, regarded to be challenging due both to the extremely high lattice mismatch (about 10%) between InSb and InP and to the possible intermixing at the interfaces[5,6] that may be intensified in this case by the incorporation competition between the group-V elements.[7] In this letter we report on the successful growth of high quality InSb/InP SPSLs. A Raman study was performed in order to investigate the Sb–P intermixing in these superlattices.

Samples were grown by atomic layer molecular beam epitaxy (ALMBE)[8] in an otherwise conventional, solid-source MBE system on semi-insulating (001) InP substrates. Typical beam equivalent pressures were $1.5-3\times10^{-6}$ Torr for both materials in the atomic layer pulsed operation mode. After oxide desorption at 490 °C under P_2 flux, the superlattices were grown at 380 °C without an intermediate buffer layer. The total thicknesses of all layers are between 0.32 and 0.8 μm using a growth velocity of 0.5 monolayers/s. The stoichiometric layer composition was controlled *in situ* by means of reflectance difference (RD) measurements of the In-dimer coverage fraction,[9] and the surface reconstruction was controlled by reflection high energy electron diffraction (RHEED). After growth the samples were cooled down under Sb pressure until 300 °C, from thereon no desorption could be observed.

We grew various $(InSb)_m(InP)_n$ SPSLs with equivalent mean compositions close to those of InP and InSb, respectively, with (m,n) equal to (1,15), (15,1), (10,1), (8,1), and (4,1). For the Sb-rich compositions, i.e., where the InSb layers are thicker than the InP layers in the superlattice and, therefore, are also thicker than 1 monolayer (ML), we observed a transition from a two-dimensional growth mode to three-dimensional island growth that was confirmed by a spotty RHEED pattern within the second InSb layer. This island growth occurs after about 1.1 ML. After further superlattice growth of approximately 200 Å the RHEED pattern progressively turned streaky again, indicating the recovery of a plane growth front. For the InP-rich samples this growth mode transition was not observed, because the InSb layer thickness here was limited to 1 ML, which is less than the critical thickness for this transition.

All the samples were studied by high resolution x-ray diffractometry (HRXRD) and Raman spectroscopy. HRXRD $\theta/2\theta$ scans were carried out in a Bede D^3 diffractometer in the high intensity mode, measuring the symmetric 004, 002, and the asymmetric 115 reflections. Figure 1 shows the 004 reflections of samples $(InSb)_{15}(InP)_1$ and $(InSb)_1(InP)_{15}$. In sample $(InSb)_{15}(InP)_1$ up to forth order satellites can be clearly seen, thus allowing accurate determination of the period thickness and average Sb content. In sample $(InSb)_1(InP)_{15}$ only second order satellites can be distinguished, mainly due to the lower total thickness of the SPSL and the lower Sb content. The other samples, except

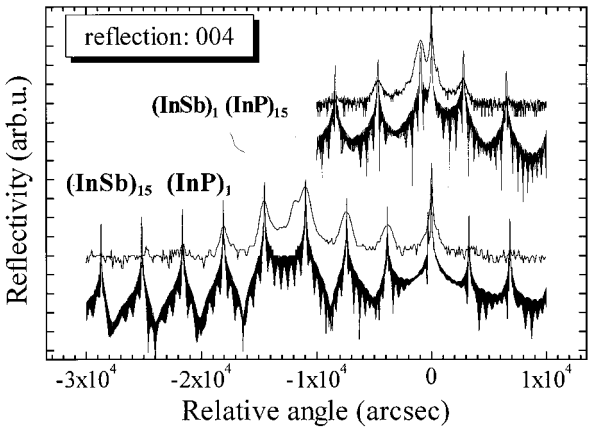

FIG. 1. HRXRD measurements and simulations of samples $(InSb)_{15}(InP)_1$ (bottom) and $(InSb)_1(InP)_{15}$ (top) taken from the (004) reflection. Satellite peaks up to fourth order around the 0-order peak can be observed.

[a]Electronic mail: thomas@imm.cnm.csic.es
[b]Present address: ETSIT, Real de Burgos, 47011 Valladolid, Spain.

TABLE I. Structural parameters of the SPSLs. R_{II} is the in-plane relaxation, a_{II} the in-plane lattice parameter, and $a_{\perp}$ the partially strained perpendicular lattice parameter. The number of monolayers was calculated by dividing the thicknesses used in the simulations by $a_{\perp}$ for each material.

Sample	R_{II} (%)	a_{II} (Å)	$a_{\perp}$ InSb (Å)	$a_{\perp}$ InP (Å)	Monolayers (InSb)/(InP)
$(InSb)_1(InP)_{15}$	4(1)	5.893(4)	7.118(6)	5.842(4)	0.96(5)/15.95(5)
$(InSb)_{15}(InP)_1$	93(1)	6.437(5)	6.526(5)	5.238(4)	14.85(5)/0.98(5)

$(InSb)_4(InP)_1$, also show satellite peaks, but the values of their half-widths are higher than those displayed in Fig. 1, explaining they are not shown here.

The experimental scans were fitted with theoretical curves obtained through our improved simulation program.[10] The results of the fits are given in Table I. The perpendicular lattice parameters $a_{\perp}$ were calculated by utilizing the conventional anisotropic elasticity theory.[11] Sample $(InSb)_1(InP)_{15}$ is almost pseudomorphic to the InP substrate (R_{II} is only 4%). On the other hand, sample $(InSb)_{15}(InP)_1$ is much more relaxed ($R_{II}=93\%$) as would be expected from its higher Sb content and thickness.

In Fig. 2 we present the Raman spectra of the $(InSb)_{15}(InP)_1$ and $(InSb)_1(InP)_{15}$ superlattices, respectively, obtained outside resonance conditions in the $z(xy)z$ configuration, thus $\{x,y,z\}$ $\{[100],[010],[001]\}$. In sample $(InSb)_{15}(InP)_1$ we observe two peaks, which we attribute to the confined longitudinal optical (LO) phonon of the strained InP layer (at 299 cm^{-1}) and to the first confined mode of the InSb layer (at 193.5 cm^{-1}). The shoulder of the last peak on its low energy side was also observed in InSb samples having similar electron concentrations, and is attributed to a plasmonlike feature. Sample $(InSb)_1(InP)_{15}$ also presents two main peaks, one corresponding to the confined phonon mode of the InP layer (at 345 cm^{-1}) and the other one to the confined InSb phonon (at 194 cm^{-1}).

The frequencies of the modes propagating along the growth direction can be calculated using a planar force constant model with interaction up to second neighboring planes. The three force constants are obtained from the frequencies $\omega_{LO}(\Gamma)$, $\omega_{LO}(X)$, and $\omega_{LA}(X)$ of the bulk material. For unstrained systems the results obtained with this simple model are close to those obtained using more sophisticated models.[12] The strain can be accounted for by assuming that the force constants are modified. This modification can be obtained in terms of the phonon deformation potential, the elastic constant of the bulk material, and the measured built-in strain.[13] We assume that the three force constants are modified in the same proportion. The phonon frequencies of the SPSLs are calculated by building a supercell using the strained force constants of the constituent layers.[10]

The calculated frequencies, using the phonon deformation potentials of Refs. 14 and 15 and the strain resulting from x-ray characterization, are given in Table II [row (a) sharp interface]. The frequencies of the phonons of the thicker layers agree with the experiment, but the phonon frequencies of the thinner layers do not. This discrepancy between theory and experiment could be due to the existence of nonsharp interfaces.[16,17] In order to quantify this effect we have assumed a certain degree of anion intermixing at the interfaces. InSbP alloys have two-mode behavior[18] and the vibrational properties of the modulated alloy system can be calculated using a modified version of the random isoamplitude model.[19] We include force constants that describe the interaction up to the second neighboring planes. Therefore, there are two first neighbor force constants: K_{In-Sb} and K_{In-P} and four second neighbor force constants: K_{In-In}, K_{Sb-Sb}, K_{P-P}, and K_{Sb-P}. All the force constants vary linearly with the composition. K_{In-In} varies linearly between the values of the two binary compounds. The values of the four independent coefficients of the linear dependence that result in this model are obtained from the frequencies of the local modes of Sb in InP and P in InSb,[18,20] and from the composition dependence of the frequencies of the Γ-related alloy modes.[18] With those assumptions a very good description of the composition dependence of the frequencies of the InSb-like and InP-like LO modes in unstrained InSbP is obtained. We assume that the strain modifies the force constants in a similar way as that for the corresponding binary compounds. The resulting force constants are used in the calculation of

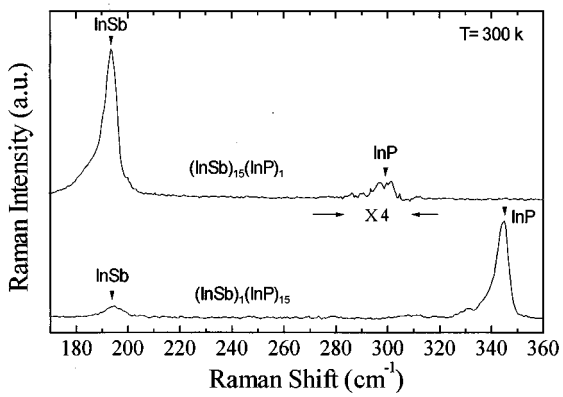

FIG. 2. Raman spectra of samples $(InSb)_{15}(InP)_1$ and $(InSb)_1(InP)_{15}$ in the $z(xy)z$ configuration outside resonance conditions. Confined phonon peaks related to InP and InSb can be observed.

TABLE II. Calculated frequencies (in cm^{-1}) for the LO phonons related to InP and InSb for samples $(InSb)_1(InP)_{15}$ and $(InSb)_{15}(InP)_1$. Three different types of interfaces are considered: (a) sharp interfaces (no intermixing); (b) short range interdiffusion, assuming a diffusion length of 1 ML monolayer; and (c) long range segregation, assuming a segregation coefficient of 85%. The experimental frequencies are also shown.

	$(InSb)_1(InP)_{15}$		$(InSb)_{15}(InP)_1$	
Interface type/$\omega(cm^{-1})$	LO (InSb)	LO (InP)	LO (InSb)	LO (InP)
(a) Sharp interfaces	204.5	342	192.5	272
(b) Interdiffusion (1 ML)	204	342.5	192.5	293
(c) Segregation (85%)	195.5	344.5	191	288.5
Experiment	194	344	193.5	299

the phonon frequencies of SPSLs including intermixing. In order to determine the peak frequency, we estimate the Raman intensity of each phonon by using the bond polarizability model[15] and we perform a convolution.

The calculated peak frequencies for two different examples of anion intermixing are included in Table II [rows (b) and (c)]. Row (b) corresponds to short range Sb–P interdiffusion,[17] assuming a diffusion length of 1 ML, and row (c) corresponds to long range segregation (carry-over),[6,18] assuming a segregation coefficient of 85%. It can be seen in Table II that the experimental data for the InP-rich sample agree very well with long range segregation. In this case the segregation of Sb may be enhanced by the very high compressive strain of the InSb layer. In addition, the calculated frequencies of InP-like modes localized in the intermixed InSb layer (not shown in Table II) are very close to the small peak observed at 332 cm^{-1} in Fig. 2. As far as the InSb-rich sample is concerned, the assessment of intermixing also clearly improves the agreement between theory and experiment, both in the case of short range interdiffusion and in the case of segregation, but it is not possible to conclusively elucidate which of the proposed types of intermixing is closer to the experimental situation.

In conclusion, we have grown $(InSb)_m(InP)_n$ short period superlattices by MBE. HRXRD measurements clearly show the periodicity of the superlattices, with observable satellite peaks up to fourth order in sample $(InSb)_{15}(InP)_1$. The Raman spectra of the superlattices show two peaks related to the confined phonons of the InSb and InP layers, respectively. The experimental Raman results strongly suggest that the interfaces between InSb and InP are not sharp.

The authors would like to gratefully acknowledge support from the HCM program (GOODS, network CT930349), and from CICYT through Project Nos. MAT 95-0966-C02-01, TIC95-0106, and TIC95-0547.

[1] C. G. Bethea, M. Y. Yen, B. F. Levine, K. K. Chor, and A. Y. Cho, Appl. Phys. Lett. **51**, 1431 (1987).
[2] R. J. Menna, D. R. Capewell, R. U. Martinelli, P. K. York, and R. E. Enstrom, Appl. Phys. Lett. **59**, 2127 (1991).
[3] T. Fukui and Y. Horikoshi, Jpn. J. Appl. Phys. **20**, 587 (1981).
[4] R. M. Biefeld, K. C. Kurtz, and D. M. Fostaedt, J. Cryst. Growth **133**, 38 (1993).
[5] J. M. Moison, C. Gille, F. Houzay, F. Barthe, and M. Van Rompay, Phys. Rev. B **40**, 6149 (1989).
[6] L. Samuelson and W. Seifert, in *Handbook of Crystal Growth*, edited by D. T. J. Hurle (Elsevier Science, Amsterdam, 1994), Vol. 3, p. 747.
[7] C. T. Foxon, B. A Joyce, and M. T. Norris, J. Cryst. Growth **49**, 774 (1980).
[8] F. Briones, L. Gonzalez, and A. Ruiz, Appl. Phys. A **49**, 729 (1989).
[9] F. Briones and Y. Horikoshi, Jpn. J. Appl. Phys. 1 **29**, 1014 (1990).
[10] A. Sanz-Hervás, M. Aguilar, J. L. Sánchez-Rojas, A. Sacedón, E. Calleja, E. Muñoz, E. J. Abril, and M. López, Appl. Phys. Lett. **69**, 1574 (1996).
[11] J. Hornstra and W. J. Bartels, J. Cryst. Growth **44**, 513 (1978).
[12] E. Molinari, S. Baroni, P. Giannozzi, and S. de Gironcoli, in *The Physics of Semiconductors*, edited by E. M. Anastassakis and J. D. Joannopoulos (World Scientific, Singapore, 1990).
[13] M. I. Alonso, P. Castrillo, G. Armelles, A. Ruiz, M. Recio, and F. Briones, Phys. Rev. B **45**, 9054 (1992).
[14] B. Jusserand and M. Cardona, in *Light Scattering in Solids V*, edited by M. Cardona and G. Güntherodt (Springer, Berlin, 1989).
[15] F. H. Pollak, in *Strained-Layer Superlattices: Physics*, edited by T. P. Pearsall (Academic, San Diego, 1990).
[16] B. Jusserand, F. Alexandre, D. Paquet, and G. Le Roux, Appl. Phys. Lett. **47**, 301 (1985).
[17] B. Jusserand and F. Mollot, Appl. Phys. Lett. **61**, 423 (1990).
[18] M. J. Jou, Y. T. Cherng, and G. B. Stringfellow, J. Appl. Phys. **64**, 1472 (1988).
[19] J. Leng, Y. Quian, P. Chen, and A. Madhukar, Solid State Commun. **69**, 311 (1989).
[20] A. S. Barker and A. J. Siervers, Rev. Mod. Phys. **47**, S1 (1975).